Newly identified *c-KIT* receptor tyrosine kinase ITD in childhood AML induces ligand-independent growth and is responsive to a synergistic effect of imatinib and rapamycin

Selim Corbacioglu, Mehtap Kilic, Mike-Andrew Westhoff, Dirk Reinhardt, Simone Fulda, and Klaus-Michael Debatin

Activating mutations of *c-KIT* lead to ligand-independent growth. Internal tandem duplications (ITDs) of exon 11, which encodes the juxtamembrane domain (JMD), are constitutively activating mutations found in 7% of gastrointestinal stromal tumors (GISTs) but have not been described in childhood acute myeloid leukemia (AML). DNA and cDNA from 60 children with AML were screened by polymerase chain reaction (PCR) for mutations of the JMD. A complex ITD *(kit cITD)* involving exon 11 and exon 12 was identified with a relative frequency of 7% (4/60). The human kit cITDs were inserted into the murine c-Kit backbone and expressed in Ba/F3 cells. KIT cITD induced factor-independent growth and apoptosis resistance, and exhibited constitutive autophosphorylation. KIT cITD constitutively activated the PI3K/AKT pathway and phosphorylated STAT1, STAT3, STAT5, and SHP-2. Imatinib (IM) or rapamycin (Rap) led to complete inhibition of growth, with IC50 values at nanomolar levels. IM and Rap synergistically inhibited growth and surmounted KIT cITD–induced apoptosis resistance. IM but not LY294002 inhibited phosphorylation of STAT3 and STAT5, suggesting aberrant cross talk between PI3K- and STAT-activating pathways. The findings presented may have immediate therapeutic impact for a subgroup of childhood AML–expressing *c-KIT* mutations. (Blood. 2006;108:3504-3513)

Introduction

The proto-oncogene *c-KIT* encodes the receptor tyrosine kinase[1] (RTK) KIT, a member of the type III RTK subfamily structurally related to the platelet-derived growth factor receptor (PDGFR) c-fms and FLT3, characterized by 5 immunoglobulin-like domains, a single transmembrane helix, a cytoplasmic juxtamembrane domain (JMD), and split kinase domain.[2,3]

KIT signaling is regulated by KIT ligand (KL). Upon binding of KL, KIT forms a homodimer, autophosphorylates tyrosine residues, and induces diverse signal transduction cascades. Phosphorylated tyrosine 567 (Tyr^{567}) and tyrosine 569 (Tyr^{569}) serve as docking sites for adapter proteins, tyrosine phosphatases SHP-1 and SHP-2, and Src family kinases.[4-6] Tyrosine residue 719 (Tyr^{719}) in the kinase insert (KI) domain interacts with the regulatory subunit p85 of the phosphoinositide-3 kinase (PI3K).[7] Activated KIT induces tyrosine phosphorylation of signal transducers and activators of transcription (STATs)[8] via either members of the JAK family or by Src family kinases directly.[9]

Through these diverse signal transduction pathways and tissue-specific regulations, *c-KIT* affects development and maintenance of several cell systems including hematopoiesis.[10-14]

Somatic mutations causing constitutive activation of KIT have been associated with a number of neoplastic conditions, including gastrointestinal stromal tumors (GISTs)[15] and leukemias.[16] KIT is expressed by myeloblasts in approximately 60% to 80% of acute myeloid leukemia (AML).[17] In AML in adults, the most common mutations involve codon 816 of the phosphotransferase domain encoded by exon 17.[18,19] Beghini et al[20] report incidences of 4% of exon 8 and 8.4% of exon 17 mutations in children with core binding factor (CBF) AML. JMD mutations encoded by exon 11 are responsible for the majority of GISTs, with a reported incidence of 7% of internal tandem duplications (ITDs) inserting 6 to 20 amino acids,[21,22] and ITDs are the most frequent activating mutations of FLT3 in adults, seen in 25% to 30% of AML.[23,24] In childhood AML, FLT3 ITDs account for 15.4% of mutations.[25] Mutations in the JMD of *c-KIT* are rare in AML of adults, with only 3 reported cases consisting of ITDs.[16,20]

The tyrosine kinase inhibitor imatinib (IM) blocks KIT activity[26] and is effective in the treatment of GISTs.[27] Nevertheless, patients develop resistance over time,[28] requiring additional agents for cure.

The serine/threonine kinase mTOR downstream of PI3K/AKT regulates cell growth and proliferation (recently reviewed by Bjornsti and Houghton[29]). Constitutively activated RTK, as well as amplification of the p110 catalytic subunit of PI3K or AKT, and loss of PTEN phosphatase (among others) alter the PI3K-mTOR pathway. The macrolide rapamycin (Rap) binds to the immunophilin FKBP12, and this complex inhibits mTOR.

Here, we report a novel *c-KIT* mutation of the JMD identified in 7% of pediatric AMLs consisting of a complex ITD involving exons 11 and 12 named *kit cITD*. *kit cITD* conferred factor-independent growth, and in comparison with wild-type kit (kit WT) the signaling properties of *kit cITD* revealed deregulated kinase activity with constitutive aberrant phosphorylation of several downstream signaling pathways. Constitutive proliferation was

From the Department of Pediatrics, University of Ulm; and Department of Pediatric Hematology and Oncology, Children's Hospital, Hannover Medical School, Germany.

Submitted May 5, 2006; accepted June 28, 2006. Prepublished online as *Blood* First Edition Paper, July 13, 2006; DOI 10.1182/blood-2006-05-021691.

The authors declare no competing financial interests.

Reprints: Selim Corbacioglu, Department of Pediatrics, University of Ulm, Eythstr 24, D-89075 Ulm, Germany; e-mail: selim.corbacioglu@uniklinik-ulm.de.

The publication costs of this article were defrayed in part by page charge payment. Therefore, and solely to indicate this fact, this article is hereby marked "advertisement" in accordance with 18 USC section 1734.

synergistically inhibited, and apoptosis resistance was also exquisitely sensitive to a combination of IM and Rap.

Patients, materials, and methods

Patients

Sixty pediatric patients with de novo AML registered in the studies AML-BFM 98 and 2000 (Berlin-Frankfurt-Münster) were included in this study. Cryopreserved marrow specimens were obtained from the AML-BFM reference laboratory after informed consent had been obtained. Study protocols AML-BFM 1998 and 2000 were approved by the Institutional Review Board of the University of Ulm, Germany.

The AML-BFM Study Group (Münster, Germany) reviewed the diagnosis of AML in these children, as well as the cell biologic data presented here (Table 1). First-line chemotherapy was given according to 2 different protocols (AML-BFM 1998, AML-BFM 2000), all based on intensive chemotherapy consisting of cytarabine plus anthracyclines.

Reagents

Recombinant murine interleukin 3 (IL-3) and recombinant murine kit ligand (KL) were purchased from PeproTech (Rocky Hill, NJ). Anti-KIT antibody (Ab-1; Oncogene, San Diego, CA), anti-p85 PI3K (Upstate Biotechnology, Lake Placid, NY), anti-AKT (BD Biosciences, Erembodegem, Belgium), anti-ERK (Sigma-Aldrich, Munich, Germany), anti–PY^{719}-KIT, anti-Pp85PI3K, anti-PS^{473}AKT, anti-p70S6K, anti-PT^{389}p70S6K, anti-S6RP, anti-$PS^{235/236}$S6RP, anti–SHP-2, anti–PY^{542}SHP-2, anti-PT^{202}/Y^{204}ERK1/2, anti-Stat1, anti-PY^{701}Stat1, anti-Stat3, anti-PY^{705}Stat3, anti-Stat5, and anti-PY^{694}Stat5 (Cell Signaling Technology, Beverly, MA) were used in Western blotting analysis as described.

IM was provided by Novartis Pharma (Basel, Switzerland); Rap was purchased from Sigma-Aldrich and LY294002, from Calbiochem (Darmstadt, Germany). The monoclonal inhibitory anti-KIT antibody ACK2 was kindly provided by Dr Peter Besmer (New York, NY).

Table 1. Clinical features and laboratory characteristics of 60 pediatric patients with AML recruited from the AML-BFM studies 1998 and 2004

Characteristic	No exon 11 cITD	kit cITD
Median age, y (range)*	10 (0.5-18.8)	13.7 (9.7-16.6)
Male/female, %*	55/45	75/25
Median WBC count, $\times 10^9$/L (range)*	66.5 (1.8-550)	21.4 (4-48)
Marrow blast, % (range)*	81 (0-98)	67 (45-89)
FAB class, no. (%)*		
M0	4 (6)	0 (0)
M1	7 (12)	0 (0)
M2	21 (39)	2 (50)
M3	2 (4)	0 (0)
M4	8 (14)	0 (0)
M5	13 (23)	2 (50)
M6	0 (0)	0 (0)
M7	1 (2)	0 (0)
Karyotype, no. (%)†		
Normal	11 (22)	0 (0)
t(15;17)	2 (4)	0 (0)
t(8;21)	10 (20)	2 (67)
t(9;11)	5 (10)	1 (33)
t(4;11)	6 (12)	0 (0)
Inv 16	2 (4)	0 (0)
Trisomy 8	2 (4)	0 (0)
−9	2 (4)	0 (0)
Other	10 (20)	0 (0)

WBC indicates white blood cell.
*For the "No exon 11 cITD" column, n = 56; for the "kit cITD" column, n = 4.
†For the "No exon 11 cITD" column, n = 50; for the "kit cITD" column, n = 3.

The FITC-conjugated rat anti–mouse KIT monoclonal antibody 2B8-APC was purchased from Pharmingen (Heidelberg, Germany).

Cell culture

The IL-3–dependent murine pro–B cell line Ba/F3[30] (kindly provided by Dr Martin Ruthardt, Frankfurt, Germany) was maintained in complete RPMI, supplemented with 10 ng/mL IL-3 (PeproTech, London, United Kingdom), 10% FCS (fetal calf serum), and antibiotics at 37°C with 5% CO_2. Mycoplasma infection reported to alter tumorigenicity[31,32] was excluded by both polymerase chain reaction (PCR) and antibody detection.

Reverse transcriptase–polymerase chain reaction (RT-PCR)

Total RNA was isolated from 10^7 leukemic blasts using RNAeasy (Qiagen, Hilden, Germany) according to the manufacturer's instructions. First-strand synthesis was performed using oligo-dT as primer at a concentration of 4 μM, a mixture of all 4 deoxynucleotides (125 μM each), and 1 U reverse transcriptase (Superscript II; Gibco BRL, Eggenstein, Germany) in a final volume of 20 μL at 42°C for 1 hour. For amplification, 1 μL of the RT reaction was used as template. Amplification was performed using the High Fidelity PCR Master kit (Roche, Mannheim, Germany) according to the manufacturer's instructions at an annealing temperature of 52°C and a 3-mM $MgCl_2$ concentration for 35 cycles. The sense primer was 5′-GTAGCTGGCATGATGTGCATTATT-3′, and the antisense primer was 5′-AGGGCTTCCCGTTCTGTCAAA-3′, yielding a 317-bp PCR product corresponding to nucleotides 1614 to 1931 of the published sequence of human *c-KIT*[3] spanning exons 10 to 13 and a second PCR product with variable lengths of up to 419 bp. Each PCR amplification was repeated at least twice with identical results. After purification of the 2 amplified bands, the PCR products were cloned into the pGEM-T Vector (Promega, Mannheim, Germany) and amplified in the bacterial strain DH5α.

Genomic DNA

Total DNA was isolated from approximately 10^7 leukemic blasts according to the manufacturer's instructions (Qiagen). For amplification, 100 ng genomic DNA was used as template. Amplification was performed as indicated in the preceding paragraph. The sense primer was 5′-CAGGTAACCATTTATTTGT-3′, and the antisense primer was 5′-TCATTGTTTCAGGTGGAAC-3′, yielding 2 fragments, a 327-bp PCR product of the published sequence of human *c-KIT* spanning exon 11 and a second PCR product with variable lengths of up to 708 bp. Each PCR amplification was repeated at least twice with identical results. After purification of the 2 amplified bands, the PCR products were cloned and amplified as indicated in the preceding paragraph.

DNA sequencing

DNA generated by RT-PCR was sequenced directly and after cloning of the PCR product. An ABI PRISM BigDye Terminator kit (Perkin-Elmer, Weiterstadt, Germany) was used according to the manufacturer's instructions. A standard cycle sequencing protocol with Taq polymerase was performed and analyzed on an automated sequencing system (ABI Prism 3700; Perkin-Elmer). For direct sequencing of the PCR products, the PCR primers were used. The cloned PCR fragments were sequenced using the M13 forward and reverse primers.

DNA constructs, expression plasmids, and stable transfection into Ba/F3 cells

The cDNA of murine *c-Kit* was kindly provided by Dr Peter Besmer (New York, NY). Three nucleotide exchanges of the subcloned PCR fragments of the human *c-KIT* cDNA were introduced by site-directed mutagenesis with Quickchange (Stratagene, La Jolla, CA): 2 in exon 10 in order to modify the amino acid code unique to exon 10 of the murine cDNA sequence introducing a *Bsa*BI site, and 1 in exon 12 introducing a *Nde*I site unique to the murine cDNA of exon 12 without alteration of the amino acid code. A *Bsa*BI/*Nde*I fragment of the PCR products spanning nt's 1633 to 1845 of the human *c-KIT* cDNA including the cITD was substitutionally introduced

into the sequence of murine *c-Kit* cDNA. The sequence of the mutants was confirmed by DNA sequencing. The constructs were cloned into an expression vector (pAL) under the control of the 59LTR of the Moloney murine sarcoma virus (MoMSV), derived from pLXSN (Clontech, Palo Alto, CA). Plasmid DNA (30 μg) of either plasmid and 3 μg pMAM/BSD (Kaken Pharmaceutical, Tokyo, Japan) were cotransfected into Ba/F3 cells by electroporation using Gene Pulser (Bio-Rad, Munich, Germany) in 0.4-cm cuvettes at 350 V and 950 μF. Cells were selected with 15 mg/mL blasticidin (Invitrogen, Groningen, the Netherlands) in IL-3–supplemented culture. Polyclonal cell lines were used for further experiments. Cell passage was limited and stability of the cell lines was confirmed via fluorescence-activated cell sorter (FACS) analysis and functional assays prior to each experiment.

^{3}H-thymidine incorporation, growth inhibition, and synergism

Assays were conducted in 96-well plates. Cells (2×10^4 Ba/F3) were added in 100 μL medium supplemented with FCS to titrated concentrations of ACK2 as indicated with maximal KL stimulation up to a total volume of 200 μL. After 48-hour incubation at 37°C, 0.37 MBq (10 μCi) ^{3}H-thymidine was added to each well 12 hours before harvesting on glass fiber filters. β-Emission of the bound DNA was analyzed with a scintillation counter. Experiments were repeated at least 3 times. Each data point represents the mean plus or minus standard deviation of 3 wells.

Growth inhibition assays were conducted with various concentrations of IM and Rap in 96-well plates for 48 hours in triplicate. The combination index[33] was determined by using CALCUSYN software (Biosoft, Cambridge, United Kingdom). IC50s for IM or Rap were calculated by sigmoidal curve–fitting software (Origin, Northampton, MA).

Cell-cycle analysis

Ba/F3 cells were incubated with inhibitors with the indicated concentrations for 24 hours and 48 hours. Cells were then washed with PBS and lysed in 0.5 mL GM solution (1.1 g/L glucose, 8 g/L NaCl, 0.4 g/L KCl, 0.39 g/L Na_2HPO_4, 0.15 g/L KH_2PO_4, 0.5 mM EDTA [ethylene-diamine-tetraacetic acid]) and 3 parts 95% ethanol. After centrifugation, the pellet was incubated in solution S (15 μg/mL propidium iodide, 50 μg/mL RNase in PBS) for 30 minutes at 37°C and for an additional hour at 4°C before flow cytometry.

Flow cytometry

Phycoerythrin-conjugated antibodies were from Pharmingen (San Diego, CA). After preincubation for 15 minutes at 4°C with mouse IgG, cells were stained with the antibodies for 1 hour at 4°C, washed twice with PBS/2% BSA, and analyzed by flow cytometry on a FACScalibur (Becton Dickinson, Heidelberg, Germany).

Immunoprecipitation and Western blot analysis

Approximately 10^7 Ba/F3 cells transfected with the indicated cDNA constructs were washed 3 times in cold PBS, starved for 5 hours in StemSpan SFEM (Stem Cell Technologies, Meylan, France), resuspended in 1 mL complete medium with or without KL (250 ng/mL) for 15 minutes at 37°C, and washed once with PBS. Cells were then lysed in 10% SDS (sodium dodecyl sulfate), 50 mM Tris-HCl (pH 6.7), 0.5 mM EDTA, 1 mM Na_3VO_4, 0.1 mM PMSF, 1 nM DTT (dithiothreitol), 10 nM ocadaic acid (Sigma-Aldrich), and proteinase inhibitor mixture (Sigma-Aldrich) for 5 minutes on ice. Cell lysates were clarified at 20 000*g* for 30 minutes. For Western blotting, lysates were heated in SDS sample buffer and separated by SDS–polyacrylamide gel electrophoresis (PAGE; 20 μg per lane). Gels were electroblotted to nitrocellulose membranes (Amersham Pharmacia Biotech, Uppsala, Sweden) and incubated with antibodies as indicated in 2% BSA/TBS-T 0.2% at 4°C overnight. Antibody binding was detected with HRP (horseradish peroxidase)–labeled secondary antibodies, followed by chemiluminescence detection (ECL-Plus system; Amersham Pharmacia Biotech). The membranes were stripped and reprobed with the protein-specific antibodies as a control for equal loading of the gel.

Rap-, IM-, and radiation-induced apoptosis

Ba/F3/kit WT cells (1×10^6) were supplemented with KL (250 ng/mL). Ba/F3/kit cITDs were maintained without KL. Apoptosis was determined by flow cytometry (FACScan; Becton Dickinson, Heidelberg, Germany) analysis of DNA fragmentation of propidium iodide–stained nuclei after incubation of Ba/F3 cells with inhibitors with the indicated concentrations for 24 hours and 48 hours.

For radiation-induced apoptosis, 1×10^6 Ba/F3/kit WT and Ba/F3/kit cITD cells were starved for 5 hours, exposed to 20 Gy γ-irradiation, and thereafter supplemented with KL (100 ng/mL) or no factor. Cell viability was analyzed using DNA fragmentation of propidium iodide–stained nuclei. Cells negative for propidium iodide were counted as viable cells.

Immunostaining and confocal microscopy

Cells were treated as indicated in the preceding paragraph. After an incubation period of 2 hours, cells were fixed with 3.7% paraformaldehyde (in PBS) for 15 minutes. Permeabilization was performed with 0.5% Triton X (in PBS). After 1 hour block in 10% FCS, the primary antibodies directed against phospho-Histone H2AX (1:100; Upstate, Hamburg, Germany) and RAD51 (1:50; Santa Cruz Biotechnology, Heidelberg, Germany) were added overnight. The secondary antibodies (Texas Red anti–rabbit IgG [Vector Laboratories, Burlingame, CA]; anti–mouse fluorescein-conjugated F(ab′)2) were used for 1 hour at a dilution of 1:100. Immunofluorescence images were captured using a laser scanning confocal microscope (Leica DM IRB; Heidelberg, Germany).

Results

Patient characteristics of the study population

The parameters of age, sex, diagnostic white blood cell count, bone marrow blast percentage, cytogenetics, and FAB classification are shown in Table 1. Three (75%) of 4 patients with activating mutations had informative cytogenetics. Two (50%) of 4 patients had favorable (t(8;21)), and 1 patient had unfavorable cytogenetics (t(9;11)). In the group of patients without *c-KIT* mutations, 50 (89%) of 56 patients had informative cytogenetics. Twenty-five (50%) of 50 had either normal (22%) or favorable (28%) cytogenetics. Eleven patients (22%) had an abnormal chromosome 11 (5 with t(9;11) and 6 with t(4;11)). Of the 4 patients, 2 patients suffered from early relapse and died. One patient is in remission and one patient was lost to follow-up.

Mutational analysis, construction, and cloning of *kit cITD* from primary pediatric AML cells

DNA and cDNA samples from peripheral blood and bone marrow of 60 patients with childhood AML were screened by PCR for mutations of exon 11. In 4 (7%) of 60 samples, we identified a novel complex ITD that consisted of fused inverted fragments from exon 12 and exon 11, inserted in-frame between exon 11 and exon 12 and translated into 24 to 34 amino acids. All cITDs consisted of identical 5′ exon 12 fragments with varying lengths of exon 11 fragments. One cITD (cITD2) had an additional P573S point mutation in the exon 11 fragment (Figure 1A).

To examine the role of *kit cITD* mutations and to study transduction pathways, we constructed mouse *c-Kit* cDNA expression mutants with inserted human kit cITD sequences (Figure 1). After introduction into Ba/F3 cells and selection of the bulk culture for 14 days in the presence of IL-3, stable expression of KIT was established. The KIT cITD mutant receptors were expressed at comparable levels with KIT WT (data not shown).

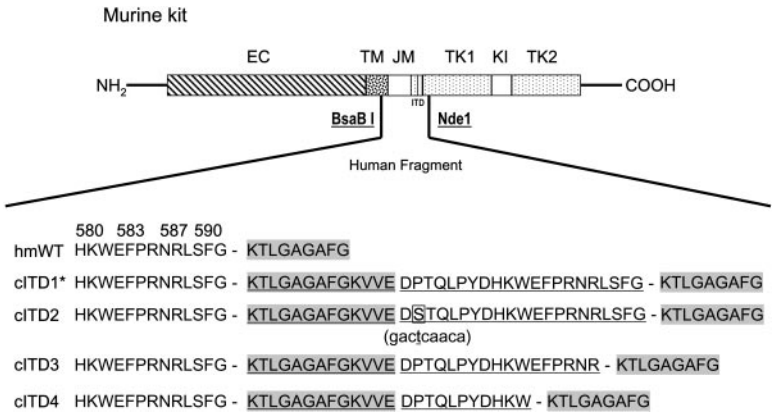

Figure 1. Schematic diagram of *kit cITDs* and their expression in Ba/F3 cells. A human *c-KIT* fragment spanning nt's 1633 to 1845, containing either wild-type or the cITD1 mutation (indexed with an asterisk), substituted the corresponding murine fragment delimited by the restriction sites *Bsa*BI and *Nde*I. The predicted amino acid sequences from either the wild-type or the 4 identified cITDs are shown. They affect amino acids 593 to 605 from exon 12 and 572 to 592 from exon 11. cITD2 has an additional P573S point mutation in the exon 11 fragment (bold and boxed; the nucleotide change in parentheses underneath is bold and underlined). Duplicated sequences are underlined; exon 12 sequences are highlighted in gray. EC indicates extracellular domain; TM, transmembrane domain; JM, juxtamembrane domain; TK, tyrosine kinase domain; KI, kinase insert; hmWT, human/mouse wild-type; and cITD, complex internal tandem duplication. The amino terminus is labeled NH_2, and the carboxy terminus is labeled COOH.

Factor-independent proliferation of Ba/F3/kit cITD

We analyzed the biologic consequences of KIT cITD by comparing the proliferative response of the kit WT–transfected Ba/F3 line (Ba/F3/kit WT) with cell lines containing the 4 kit cITD variants (Ba/F3/kit cITDs 1 to 4). Proliferation was analyzed by ^{3}H-thymidine incorporation. In contrast to Ba/F3/kit WT, the Ba/F3/kit cITD variants proliferated independently of KL (Figure 2) or IL-3 (data not shown), comparable with Ba/F3/kit WT stimulated with maximal levels of KL or IL-3 (10 ng/mL) (data not shown), and could not be inhibited with the anti-KIT antibody ACK2 (Figure 2).

Constitutive and ligand-independent activation and downstream signaling pathways induced by KIT cITD

To analyze the signaling properties of KIT cITD in comparison with WT receptor, we first studied the autophosphorylation status of KIT cITD and the phosphorylation status of p85PI3K comparing Ba/F3/kit WT with the Ba/F3/kit cITD variants. Total cell lysates were subjected to immunoblotting with antibodies specific for the activation status of the involved signal transduction molecules, verifying the loading conditions by antibodies detecting the molecules independent of their activation state. All 4 KIT cITD variants induced constitutive phosphorylation of the fully glycosylated receptor $p160^{kit}$, the incompletely processed internalized form, $p145^{kit}$ of PY^{719} KIT, and the regulatory subunit p85 of PI3K (Figure 3A). Since all 4 KIT cITD variants induced a constitutive phosphorylation of PY^{719} KIT and of p85, the variant with the longest involvement of exon 12 and exon 11 (cITD1) was compared with blasticidin vector mock-transfected Ba/F3 cells (Ba/F3 BSD) and Ba/F3/kit WT in order to examine the major downstream signaling pathways.

As shown in Figure 3B, AKT, S6K, and S6RP were constitutively phosphorylated in Ba/F3/kit cITD in contrast to ERK1/2, which was activated KL dependently. Taken together, cITD induced factor-independent autophosphorylation of the mature and immature forms of KIT and constitutively activated the PI3K/AKT/mTOR pathway. Activation of the MAPK pathway remained KL dependent.

Constitutive activation of STAT1, STAT3, STAT5, and SHP-2 in Ba/F3/kit cITD

In order to study aberrant phosphorylation, we also examined STAT1, STAT3, STAT5, and SHP-2 (Figure 3C). In Ba/F3/kit WT, we detected only weak phosphorylation of STAT1 and STAT3 and no phosphorylation of STAT5 when cells were starved and de novo stimulated. Ba/F3/kit cITD strongly phosphorylated all 3 STATs. No difference in SHP-1 phosphorylation was observed (data not shown). While in KIT WT, SHP-2 was not phosphorylated, Ba/F3/kit cITD cells exhibited strong constitutive phosphorylation of SHP-2. We conclude that STAT1, STAT3, STAT5, and SHP-2 are preferentially activated by KIT cITD.

IM and Rap synergistically inhibit KIT cITD–induced proliferation

Since IM and Rap have been shown to inhibit proliferation of leukemia cells with RTK gain-of-function mutants,[34] we analyzed the effect of IM or Rap on cell growth. All Ba/F3/kit cITD variants exhibited comparably strong sensitivity to inhibition by IM and Rap with IC50s similar to Ba/F3/kit WT of 30 nM and 3 nM, respectively. As a control, we used LY294002, the inhibitor of the p110 catalytic subunit of PI3K, which inhibited proliferation with comparable IC50s (2.5 μM) (Figure 4A).

In order to assess synergism, Ba/F3/kit cITDs were exposed to varying concentrations of IM and Rap at a constant ratio of 1000:1. The combination of IM and Rap markedly decreased proliferation. The doses of Rap that caused profound inhibition when used in

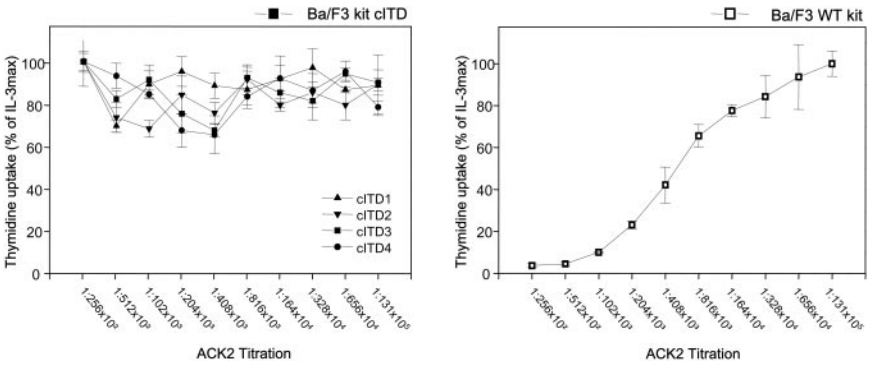

Figure 2. Ligand-independent thymidine incorporation. Cells were starved for 12 hours from IL-3 and maximally stimulated with KL 500 ng/mL. The inhibitory monoclonal antibody ACK2 was titrated as indicated. Data are shown as percentage of thymidine incorporation compared with thymidine incorporation of the respective cell line under IL-3 stimulation. Error bars indicate the standard deviation.

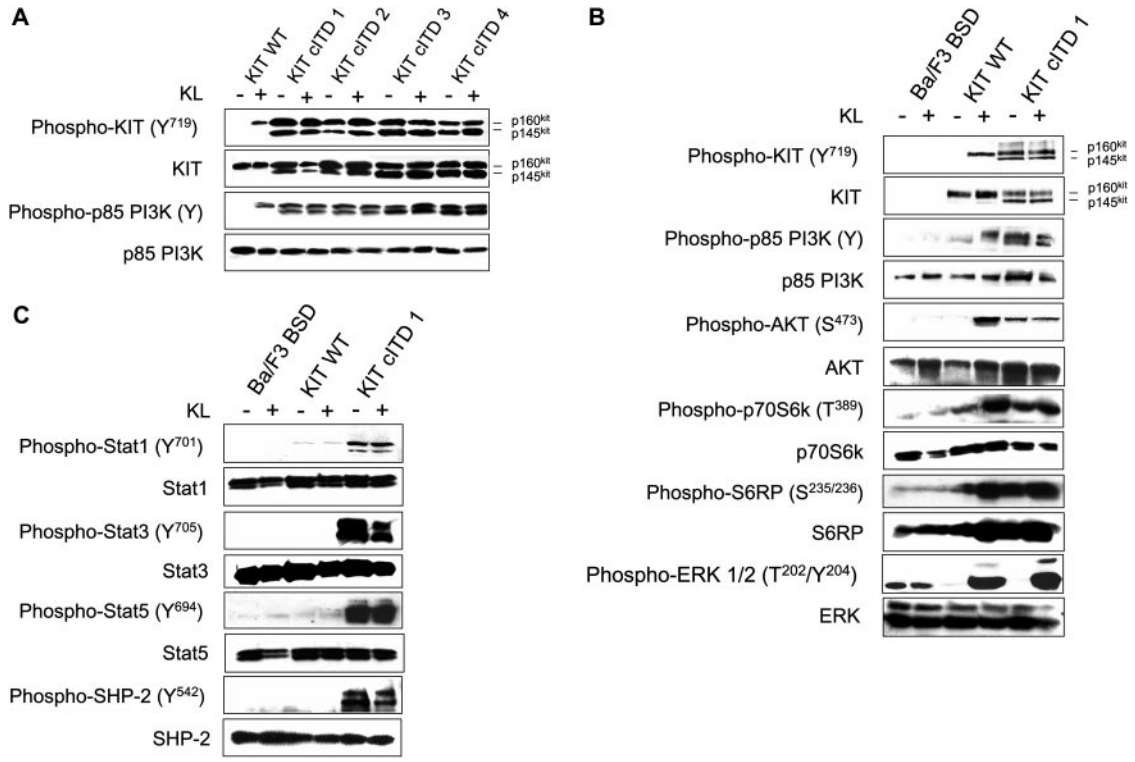

Figure 3. Constitutive tyrosine phosphorylation of KIT cITD, and ligand-independent constitutive phosphorylation of the PI3K/AKT/mTOR pathway, STAT1, STAT3, STAT5, and SHP-2. (A) Phosphorylation status of the KIT WT receptor and p85 PI3K with and without KL was determined by Western blot analysis and compared with the 4 KIT cITD variants. After a 5-hour starvation period, 1×10^7 cells were stimulated for 15 minutes in 1 mL medium with or without 250 ng/mL KL as indicated. Whole-cell lysates (20 μg per lane) were subjected to SDS-PAGE and immunoblotted with anti–phospho-specific antibodies as indicated. Phospho-KIT (Y^{719}) recognizes KIT phosphorylated on Tyr^{719}; phospho-p85 PI3K recognizes the phosphorylated regulatory subunit p85 of PI3K. (B) Phosphorylation and downstream signaling targets of WT KIT and KIT cITD1 were determined by Western blot analysis. Phospho-Akt (S^{473}) is specific for AKT phosphorylated on serine 473; phospho-p70S6k (T^{389}) is specific for p70S6K phosphorylated on tyrosine 389; phospho-S6RP ($S^{235/236}$) recognizes S6RP phosphorylated on serine 235/236; and phospho-ERK 1/2 (T^{202}/Y^{204}) is specific for the subunits p42 and p44 of the MAP kinases ERK1 and ERK2 phosphorylated on threonine 202 and tyrosine 204. Subsequently, the blots were stripped and stained with the indicated protein-specific antibodies to demonstrate equal loading. Ba/F3 BSD indicates mock-transfected Ba/F3 cells. (C) Phospho-STAT1 (Y^{701}) recognizes phosphorylated STAT1 on tyrosine 701; phospho-STAT3 (Y^{705}) recognizes STAT3 phosphorylated on tyrosine 705; and phospho-STAT5 (Y^{694}) recognizes STAT5 phosphorylated on tyrosine 694. Phospho–SHP-2 (Y^{542}) is specific for SHP-2 phosphorylated on tyrosine 542. Subsequently, the blots were stripped and stained with the indicated protein-specific antibodies to demonstrate equal loading. Ba/F3 BSD indicates mock-transfected Ba/F3 cells.

combination with IM, were far below therapeutic serum levels of 5 to 10 nM. Drug interaction analyses indicated that inhibition was synergistic (Figure 4B).

A combination of IM and Rap can overcome apoptosis resistance induced by *kit cITD*

Proliferation inhibition could reflect cell-cycle arrest and/or cell death. We therefore analyzed the cell-cycle distribution and the role of cITD in IM- and Rap-induced apoptosis. IM or Rap alone induced G_1 arrest with little apoptosis in KIT cITD–expressing cells in contrast to KIT WT, which exhibited a high DNA content in the sub-G_1 fraction. The combination increased the sub-G_1 fraction in mutant KIT–expressing cells substantially (Table 2). Apoptosis resistance was confirmed by measurement of DNA fragmentation. Again, only a combination of both drugs could increase the apoptotic cell fraction in Ba/F3/kit cITD. Individual proapoptotic effects of both drugs on Ba/F3/kit cITD and Ba/F3/kit WT were comparable with LY294002, but when combined they exceeded the effects of LY294002 (Figure 5).

Resistance to radiation-induced apoptosis of Ba/F3/kit cITD is associated with recruitment of γ-H2AX and RAD51 repair factors to nuclear foci after DNA damage

In order to further analyze mechanisms of apoptosis resistance induced by *kit cITD* and to define the role of constitutively phosphorylated STAT5, we first examined sensitivity of Ba/F3/kit cITD to γ-irradiation–induced apoptosis. Ba/F3/kit WT cells were highly sensitive to γ-irradiation, with less than 20% viability after 24 hours that could be partially rescued with KL. *kit cITD* induced an almost complete resistance to irradiation-induced apoptosis independent of cytokine substitution (Figure 6A). We compared γ-H2AX and RAD51 expression before and after irradiation-induced DNA damage. Figure 6B represents an immunostaining with antibodies directed against γ-H2AX (green) and RAD51 (red), where in unirradiated cells very few of the RAD51 foci overlap with γ-H2AX foci. After 20 Gy irradiation and 2 hours recovery, Ba/F3/kit cITD showed a strong immunostaining of RAD51 and a colocalization of RAD51 with γ-H2AX spots compared with Ba/F3/kit WT.

IM inhibits constitutively activated STAT3 and STAT5, suggesting aberrant cross talk with STAT-activating pathways

Synergism was observed when IM and Rap were combined that cannot be explained with inhibition of the PI3K/AKT/mTOR pathway alone. We investigated therefore the involvement of alternative downstream pathways and compared the phosphorylation of KIT, AKT, PI3K, p70S6K, STAT3, STAT5, and ERK in cells treated with IM, Rap, a combination of both, or LY294002. Imatinib and the combination of IM and Rap strongly inhibited the phosphorylation of KIT Y^{719}, p85, AKT, and STAT5. As expected,

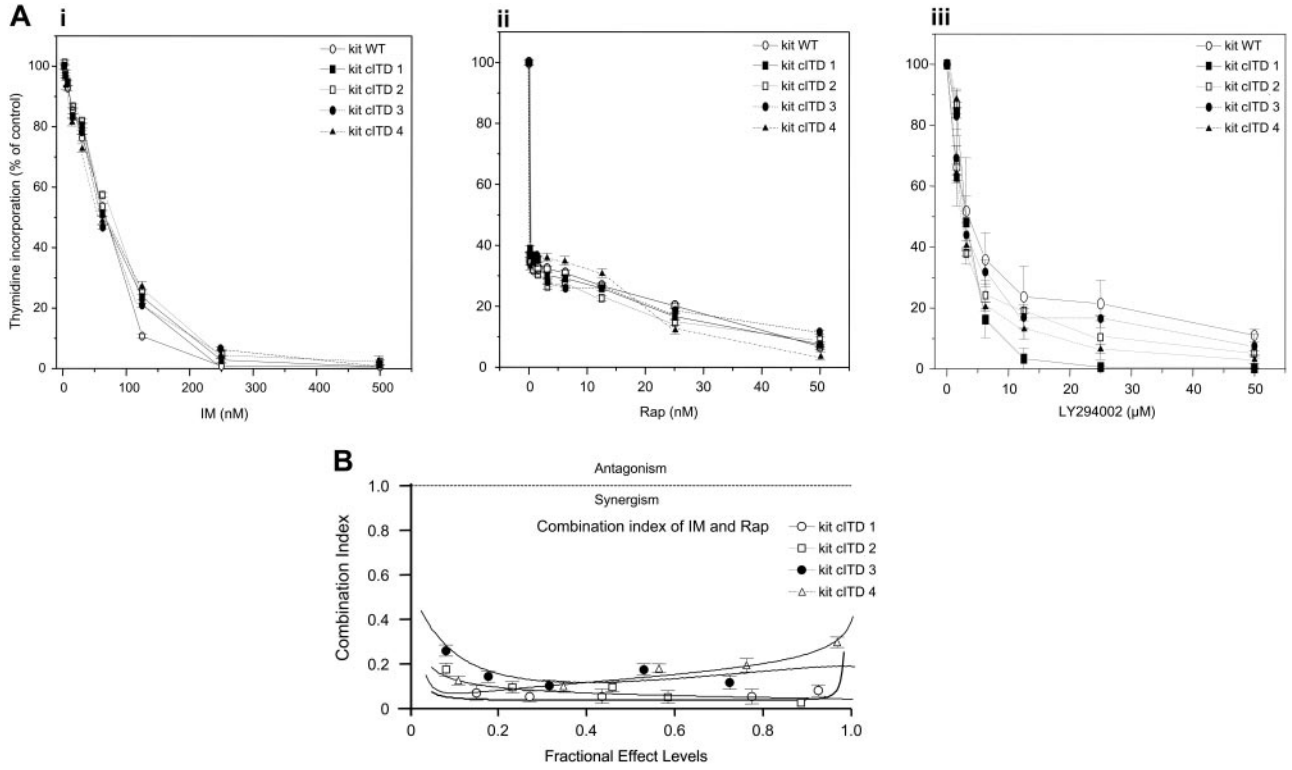

Figure 4. IM and Rap synergistically inhibit the proliferation of Ba/F3/kit cITD. (A) Ba/F3/kit WT and Ba/F3/kit cITD cells were treated with the indicated doses of (i) IM, (ii) Rap, and (iii) LY294002 for 48 hours. ^{3}H-thymidine incorporation was determined. Control cells were treated with DMSO (dimethyl sulfoxide) vehicle. (B) Ba/F3/kit cITD cells were exposed to varying concentrations of IM and Rap at a constant ratio of 1000:1 for 48 hours. Proliferation was assessed by ^{3}H-thymidine incorporation. The combination index was determined. Values below 1.0 correspond to synergy, with values below 0.3 corresponding to very strong synergy. Points are the mean of triplicate determinations; bar, ± SD.

LY294002 had no effect on PY^{719} KIT but markedly inhibited the phosphorylation of AKT in KIT WT and was less pronounced in KIT cITD. LY294002, Rap, and the combination of IM and Rap, but not IM alone, blocked the phosphorylation of p70S6K. In contrast to LY294002 and Rap, IM completely abolished the phosphorylation of STAT3. This effect was antagonized when IM was combined with Rap. Constitutive STAT5 phosphorylation could not be blocked by the Src family kinase inhibitors SU6656 and PP2 (data not shown). Activation of the MAPK pathway with its downstream target ERK in Ba/F3/kit WT and cITD is KL dependent. In Ba/F3/kit WT, ERK phosphorylation was not affected by the inhibitors. In Ba/F3/kit cITD, IM, Rap, and a combination of both drugs abolished ERK phosphorylation. In contrast, Ly294002 seemed to induce ERK phosphorylation (Figure 7).

Discussion

This is the first report of a novel mutation of the JMD of c-kit encoded by exons 11 and 12 termed *kit cITD*, which was identified in 7% of patients with pediatric AML, consisting of large fused inverted fragments inserted between exons 11 and 12. The *c-KIT*

Table 2. Cell-cycle distribution of Ba/F3/kit WT and Ba/F3/kit cITD treated with IM and Rap

	Ba/F3/kit WT				Ba/F3/kit cITD1			
	Viable cells in phase, %			Total apoptotic cells, %	Viable cells in phase, %			Total apoptotic cells, %
Drugs treated	G_1	S	G_2/M		G_1	S	G_2/M	
DMSO, control								
24 h	45.8	29.7	22.9	1.6	46.4	23.7	27.1	2.8
48 h	47.2	27.1	23.3	2.4	43.7	23.7	29.2	3.4
50 nM IM								
24 h	68.6	7.0	7.2	17.2	46.6	27.2	21.3	4.9
48 h	46.1	2.2	3.8	47.9	60.6	16.7	18	4.7
5 nM Rap								
24 h	44.4	25.2	19	11.4	57.4	19.8	17	5.8
48 h	48.9	14.7	11.3	25.1	72.1	9.1	9.5	9.3
50 nM IM and 5 nM Rap								
24 h	68.6	7.03	7.2	17.1	68.1	5.9	11.7	14.3
48 h	46.1	2.2	3.78	47.9	46	2.2	3.8	48

Ba/F3 WT and Ba/F3 kit cITD cells were treated with the indicated doses of IM and Rap, alone and in combination for 24 hours and 48 hours, respectively. Apoptosis was determined via analysis of DNA fragmentation of propidium iodide-stained nuclei.

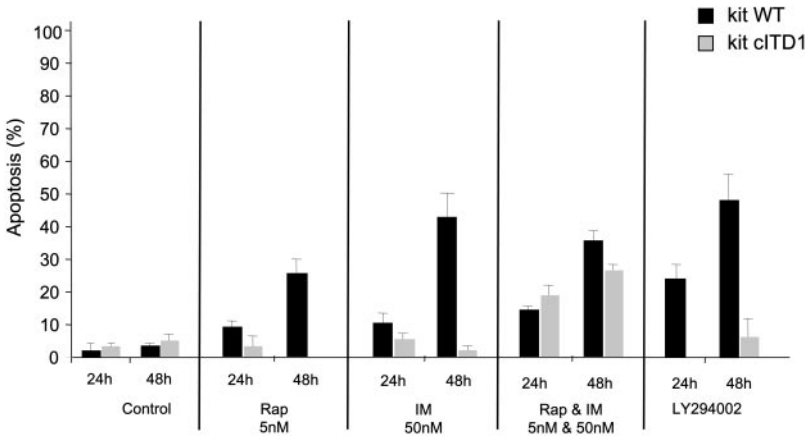

Figure 5. KIT cITD induces apoptosis resistance when treated with IM, Rap, and LY294002 in transformed Ba/F3 cells that can be overcome by a combination of IM and Rap. Ba/F3 WT and Ba/F3 kit cITD cells were treated with the indicated doses of IM and Rap (alone and in combination) and LY294002, for 24 hours and 48 hours. Apoptosis was determined via analysis of DNA fragmentation of propidium iodide–stained nuclei. Error bars indicate standard deviation.

ITD described here differs from all known *c-KIT* mutations in humans. In GISTs, *c-KIT* ITDs were identified in 7% of *c-KIT* mutations involving exclusively the 3′ end of exon 11[21] like the 3 identified c-kit ITDs in adult AML.[16,20] FLT3 ITDs are detectable in about 20% of adult AMLs. Except for one large complex ITD, all FLT3 ITDs are reported within exon 11.[35] In adult AML, *c-KIT* mutations have been preferentially associated with CBF leukemias.[16,18,36] In our series, only 2 of 3 patients with a known karyotype had a t(8;21) and 1 patient had a t(9;11) closely related to myelomonocytic and monocytic leukemias. When expressed in Ba/F3 cells, all KIT cITD variants elicited transforming ability, and induced factor-independent growth and constitutive autophosphorylation as

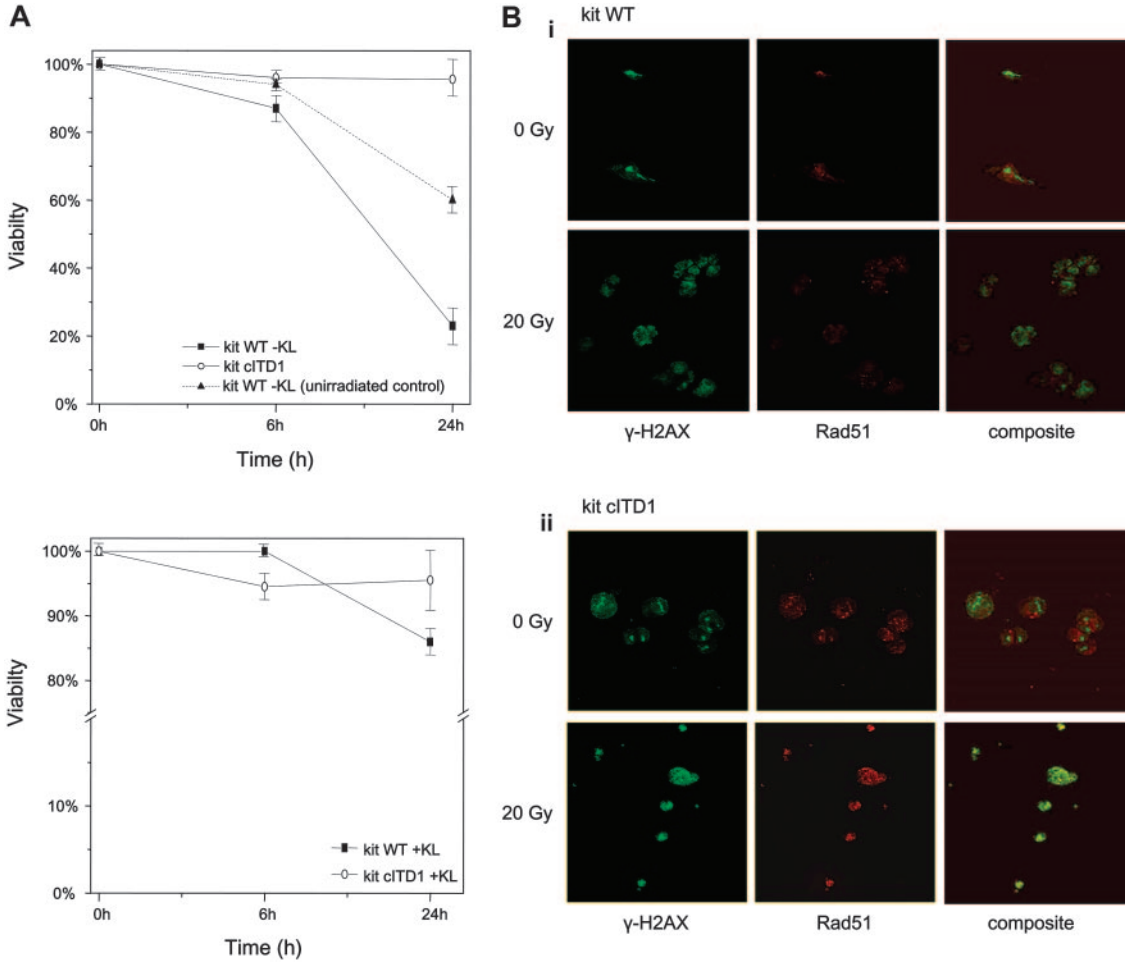

Figure 6. KIT cITD induces ligand-independent resistance against radiation-induced apoptosis and recruitment of γ-H2AX and RAD51 repair factors to nuclear foci after DNA damage. (A) Cells were starved for 2 hours and exposed to 20 Gy γ-irradiation. Cells that were propidium iodide negative were counted as viable cells. Viability was calculated as a percentage of these cells over the total cell population. KL concentration was 100 ng/mL. Unirradiated and KL-starved Ba/F3/kit WT cells were used as control. Error bars indicate standard deviation. (B) After exposure to 20 Gy γ-irradiation and recovery for 2 hours, Ba/F3/kit WT and Ba/F3/kit cITD cells were fixed, permeabilized, and stained with primary antibodies directed against γ-H2AX (green) and RAD51 (red). Subpanels Bi and Bii represent Ba/F3/kit WT and Ba/F3/kit cITD cells, respectively, stained with anti–γ-H2AX, anti-RAD51, and composite before and after γ-irradiation. Micrograph images were visualized with a Leica HCX 40×/0.85 objective lens, digitally acquired through Leica Application Suite software, and processed with Adobe Photoshop 7.0 software (Adobe Systems, San Jose, CA).

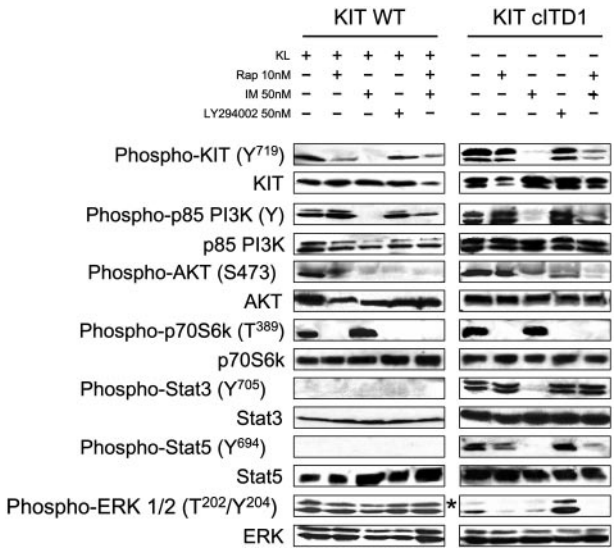

Figure 7. IM inhibits KIT cITD–induced ligand-independent constitutive tyrosine phosphorylation of STAT3 and STAT5 in Ba/F3/kit cITD. Phosphorylation status of the KIT downstream signaling targets was determined by Western blot analysis after inhibition with IM, Rap, and Ly294002. After a 5-hour starvation period, 1×10^7 cells were stimulated for 6 hours in 1 mL medium with or without 250 ng/mL KL and inhibitors at concentrations as indicated. Whole-cell lysates (20 μg per lane) were subjected to SDS-PAGE and immunoblotted with anti–phospho-specific antibodies as indicated. Phospho-KIT (Y^{719}) recognizes KIT phosphorylated on Tyr^{719}; phospho-p85 PI3K recognizes the phosphorylated regulatory subunit p85 of PI3K; phospho-Akt (S^{473}) is specific for AKT phosphorylated on serine 473; phospho-p70S6K (T^{389}) is specific for p70S6K phosphorylated on tyrosine 389; phospho-STAT3 (Y^{705}) recognizes STAT3 phosphorylated on tyrosine 705; phospho-STAT5 (Y^{694}) recognizes STAT5 phosphorylated on tyrosine 694; and phospho-ERK 1/2 (T^{202}/Y^{204}) is specific for the subunits p42 and p44 of the MAP kinases ERK1 and ERK2 phosphorylated on threonine 202 and tyrosine 204. Subsequently, the blots were stripped and stained with the indicated protein-specific antibodies to demonstrate equal loading. *Ba/F3/kit cITD stimulated with 250 ng/mL KL for 15 minutes.

well as constitutive phosphorylation of p85, the regulatory subunit of PI3K. KIT cITD induced a constitutive activation of the PI3K/AKT/mTOR pathway, confirming an essential contribution to the transformation phenotype. Tyrosine phosphorylation of p85 in Jurkat cells correlated with proliferation independently of PI3K activation, but, in contrast to our results, LY294002 could not inhibit cell growth significantly in the Jurkat cell system.[37] In cancer cells, AKT activation is associated with increased resistance to apoptosis induced by TRAIL/APO-2L,[38-41] and it inactivates several proapoptotic factors,[42] thereby promoting survival signals of many receptors, including KIT.[43] LY294002 inhibited proliferation but only partially blocked AKT phosphorylation. As a single agent, LY294002 was not able to overcome apoptosis resistance, indicating activation of several LY294002-insensitive antiapoptotic pathways in *kit cITD*. ERK1/2 remained KL inducible as has been shown for other gain-of-function mutations of KIT.[44,45] Constitutive activation of the Ras-Raf-MAP kinase pathway neither is a constant observation in gain-of-function mutations of RTK nor does it correlate with the type of mutation.[44,46,47]

We could not detect any significant activation of STAT1, STAT3, and STAT5 in Ba/F3/kit WT with KL at optimal concentrations, similar to other studies with no measurable interaction between KL/KIT and STATs.[48-50] However Ba/F3/kit cITD exhibited constitutive tyrosine phosphorylation of STAT1, STAT3, STAT5, and SHP-2 to levels not observed in maximally KL-stimulated cells expressing KIT WT. Aberrant downstream phosphorylation in gain-of-function mutations of KIT was reported frequently.[45,47,51,52] Constitutive activation of STAT proteins is found in a wide variety of malignancies,[53] and activation of STAT3 or STAT5 induced cellular transformation.[54,55] The activation pattern of STATs in gain-of function mutants is not constant with activation of STAT1, STAT3, and STAT5 in various combinations.[44,47,48,51,52] In a breast cancer model, constitutive activation of PI3K was observed to bypass AKT and p70S6K with aberrant activation of PAK, Rac, and p38 MAPK.[56] The underlying molecular mechanisms responsible for altered cellular behavior remain largely undefined. Differences in the phosphorylation pattern could be due to the cell line used but might reflect an activation pattern of a specific mutation, thus profoundly modifying the phenotype distinguishable from WT and other activating mutations.

KIT cITD induced resistance to radiation-induced apoptosis and was associated with strong nuclear colocalization of RAD51 with γ-H2AX. In FLT3 ITD mutants, hyperactivation of STAT5 induced up-regulation of its target RAD51.[57] RAD51 colocalizes with phosphorylated H2AX (γ-H2AX) and forms nuclear foci as a response to double-strand breaks in genomic DNA.[58] Therefore, radiation resistance may be the consequence of an increased activity of the gene repair machinery represented by a prominent complex formation of RAD51 with γ-H2AX.[58]

Most importantly, constitutive proliferation and apoptosis resistance of Ba/F3/kit cITD cells could be abrogated by treatment with IM and Rap. The partially inhibitory effect of IM was synergistically complemented by Rap. Synergism was also demonstrated in BCR/ABL-transformed myeloid and lymphoid cells.[34] IM is a potent inhibitor of KIT JMD mutants,[26,44] and mTOR in complex with rictor was shown to phosphorylate AKT and can therefore modulate signaling further upstream.[59] The observed partial inhibition of AKT phosphorylation by Rap in KIT WT could be due to indirect inhibition of the rictor-mTOR complex formation via substrate depletion.[59,60] This is supported by the lack of inhibition of Rap on the level of p85, but Rap did not affect phosphorylation of AKT in KIT MUT. Therefore this mechanism cannot serve as a possible explanation for the observed synergism, which remains difficult to explain with inhibition of the PI3K/AKT/mTOR pathway at different levels alone. We therefore assessed the phosphorylation pattern of the signaling molecules aberrantly activated by KIT cITD after treatment with IM, Rap, LY294002, and a combination of IM and Rap.

In *kit cITD*, IM inhibited not only the PI3K/AKT/mTOR pathway but also aberrantly activated STATs. In contrast, LY294002 could not block phosphorylation of STAT3 and STAT5. Usually STATs can be activated either through the canonical JAK pathway[4] or by Src kinases directly.[9] Parental Ba/F3 cells when stimulated with IL-3 induced phosphorylation of STAT5. This could not be inhibited with IM, indicating that the inhibitory effect of IM might be KIT cITD dependent. In BCR-ABL–positive cells, IM strongly suppressed STAT5 tyrosine phosphorylation[61] and blocked constitutive STAT3 phosphorylation in a kinase domain mutation of *c-KIT*.[45] Brizzi et al[8] removed the kinase insert domain, including the binding site for p85 that completely abrogated STAT activation, supporting a possible role of p85 in STAT phosphorylation. Whether the deletion of Y^{719}, the binding site for p85 in KIT cITD, abrogates the activation of STAT family members is the subject of ongoing research. Physiologically, the JMD of KIT appears to mediate autoinhibitory function through conformational changes of a predicted inhibitory α-helix, blocking ligand-independent dimerization and activation,[62,63] which could be disturbed by cITD inducing constitutive autophosphorylation of the cytoplasmic tail. Located also within the JMD are Tyr^{567} and Tyr^{569}, the primary sites of in vivo autophosphorylation,[62] as well as crucial binding sites for

Src kinases[4,6] and the tyrosine phosphatases SHP-1 and SHP-2.[5] Somatic mutations of SHP-2 encoded by PTPN11 were identified in juvenile and childhood leukemias.[64] In our model, SHP-2 was aberrantly activated and could therefore also influence the KIT cITD phenotype. In FLT3 ITDs, all tyrosine residues were replaced by phenylalanine and showed that ligand-independent proliferation persisted.[65] Forced dimerization of KIT induced autophosphorylation and proliferation,[66] but other characteristics of oncogenic transformation and aberrant substrate activation leading to apoptosis resistance were not investigated.

The phosphorylation pattern of ERK1/ERK2 in KIT WT– and KIT cITD–expressing cells differed after treatment with the inhibitors. Wandzioch et al[67] observed differential activation pattern of ERK in hematopoietic stem cell (HSC) lines and more committed hematopoietic precursors, indicating a molecular signaling switch that occurs during differentiation. The aberrant activation of ERK described here differs from the HSC type and the more mature hematopoietic cell–type activation pattern described above. The impression that LY294002 increased ERK phosphorylation was also observed in a human umbilical vein endothelial cell (HUVEC) system when stimulated with fibroblast growth factor 2.[68] The authors suggested a cross talk between PI3K/AKT and ERK pathways via protein kinase C (PKC).

In summary, we identified a novel complex ITD of KIT in childhood AML that induced ligand-independent growth, apoptosis resistance, and altered downstream signaling pathways. A combination of IM and Rap synergistically inhibited proliferation and apoptosis resistance. Inhibitors of signal transduction such as IM, Rap, and Ly294002 exert their effects differentially on KIT WT– and KIT cITD–expressing cells, most probably due to aberrant communication between pathways. Further work in tissue-specific cell systems is necessary in order to elucidate the characteristics of cITD-dependent signaling pathways in more detail and to improve our understanding of communicating signaling pathways and mechanisms of synergy between specific inhibitors for future therapeutic application in leukemias with *c-KIT* mutations.

Acknowledgments

We would like to thank Yvonne Sauter and Tobias Wagner for excellent technical assistance, Stavros Giagkousiklidis for technical support, and other members of the Debatin lab for helpful discussion. We also gratefully acknowledge H. Serve (Wilhelms Universität, Münster, Germany) for providing transfection constructs, M. Ruthardt (University of Frankfurt, Frankfurt, Germany) for the Ba/F3 cell line, and Novartis (Basel, Switzerland) for imatinib mesylate.

References

1. Besmer P, Murphy JE, George PC, et al. A new acute transforming feline retrovirus and relationship of its oncogene v-kit with the protein kinase gene family. Nature. 1986;320:415-421.
2. Qiu FH, Ray P, Brown K, et al. Primary structure of c-kit: relationship with the CSF-1/PDGF receptor kinase family: oncogenic activation of v-kit involves deletion of extracellular domain and C terminus. EMBO J. 1988;7:1003-1011.
3. Yarden Y, Kuang WJ, Yang-Feng T, et al. Human proto-oncogene c-kit: a new cell surface receptor tyrosine kinase for an unidentified ligand. EMBO J. 1987;6:3341-3351.
4. Linnekin D, Mou S, Deberry CS, et al. Stem cell factor, the JAK-STAT pathway and signal transduction. Leuk Lymphoma. 1997;27:439-444.
5. Kozlowski M, Larose L, Lee F, Le DM, Rottapel R, Siminovitch KA. SHP-1 binds and negatively modulates the c-Kit receptor by interaction with tyrosine 569 in the c-Kit juxtamembrane domain. Mol Cell Biol. 1998;18:2089-2099.
6. Price DJ, Rivnay B, Fu Y, Jiang S, Avraham S, Avraham H. Direct association of Csk homologous kinase (CHK) with the diphosphorylated site Tyr568/570 of the activated c-KIT in megakaryocytes. J Biol Chem. 1997;272:5915-5920.
7. Serve H, Yee NS, Stella G, Sepp-Lorenzino L, Tan JC, Besmer P. Differential roles of PI3-kinase and Kit tyrosine 821 in Kit receptor-mediated proliferation, survival and cell adhesion in mast cells. EMBO J. 1995;14:473-483.
8. Brizzi MF, Dentelli P, Rosso A, Yarden Y, Pegoraro L. STAT protein recruitment and activation in c-Kit deletion mutants. J Biol Chem. 1999;274:16965-16972.
9. Yu CL, Meyer DJ, Campbell GS, et al. Enhanced DNA-binding activity of a Stat3-related protein in cells transformed by the Src oncoprotein. Science. 1995;269:81-83.
10. Ashman LK. The biology of stem cell factor and its receptor C-kit. Int J Biochem Cell Biol. 1999;31:1037-1051.
11. Besmer P, Manova K, Duttlinger R, et al. The kit-ligand (steel factor) and its receptor c-kit/W: pleiotropic roles in gametogenesis and melanogenesis. Dev Suppl. 1993:3;125-137.
12. Nocka K, Majumder S, Chabot B, et al. Expression of c-kit gene products in known cellular targets of W mutations in normal and W mutant mice: evidence for an impaired c-kit kinase in mutant mice. Genes Dev. 1989;3:816-826.
13. Simmons PJ, Aylett GW, Niutta S, To LB, Juttner CA, Ashman LK. c-kit is expressed by primitive human hematopoietic cells that give rise to colony-forming cells in stroma-dependent or cytokine-supplemented culture. Exp Hematol. 1994;22:157-165.
14. Ishikawa K, Komuro T, Hirota S, Kitamura Y. Ultrastructural identification of the c-kit-expressing interstitial cells in the rat stomach: a comparison of control and Ws/Ws mutant rats. Cell Tissue Res. 1997;289:137-143.
15. Hirota S, Isozaki K, Moriyama Y, et al. Gain-of-function mutations of c-kit in human gastrointestinal stromal tumors. Science. 1998;279:577-580.
16. Wang YY, Zhou GB, Yin T, et al. AML1-ETO and C-KIT mutation/overexpression in t(8;21) leukemia: implication in stepwise leukemogenesis and response to Gleevec. Proc Natl Acad Sci U S A. 2005;102:1104-1109.
17. Ikeda H, Kanakura Y, Tamaki T, et al. Expression and functional role of the proto-oncogene c-kit in acute myeloblastic leukemia cells. Blood. 1991;78:2962-2968.
18. Beghini A, Larizza L, Cairoli R, Morra E. c-kit activating mutations and mast cell proliferation in human leukemia. Blood. 1998;92:701-702.
19. Ashman LK, Ferrao P, Cole SR, Cambareri AC. Effects of mutant c-kit in early myeloid cells. Leuk Lymph. 2000;37:233-243.
20. Beghini A, Ripamonti CB, Cairoli R, et al. KIT activating mutations: incidence in adult and pediatric acute myeloid leukemia, and identification of an internal tandem duplication. Haematologica. 2004;89:920-925.
21. Antonescu CR, Sommer G, Sarran L, et al. Association of KIT exon 9 mutations with nongastric primary site and aggressive behavior: KIT mutation analysis and clinical correlates of 120 gastrointestinal stromal tumors. Clin Cancer Res. 2003;9:3329-3337.
22. Heinrich MC, Corless CL, Demetri GD, et al. Kinase mutations and imatinib response in patients with metastatic gastrointestinal stromal tumor. J Clin Oncol. 2003;21:4342-4349.
23. Yokota S, Kiyoi H, Nakao M, et al. Internal tandem duplication of the FLT3 gene is preferentially seen in acute myeloid leukemia and myelodysplastic syndrome among various hematological malignancies: a study on a large series of patients and cell lines. Leukemia. 1997;11:1605-1609.
24. Yamamoto Y, Kiyoi H, Nakano Y, et al. Activating mutation of D835 within the activation loop of FLT3 in human hematologic malignancies. Blood. 2001;97:2434-2439.
25. Liang DC, Shih LY, Hung IJ, et al. FLT3-TKD mutation in childhood acute myeloid leukemia. Leukemia. 2003;17:883-886.
26. Heinrich MC, Griffith DJ, Druker BJ, Wait CL, Ott KA, Zigler AJ. Inhibition of c-kit receptor tyrosine kinase activity by STI 571, a selective tyrosine kinase inhibitor. Blood. 2000;96:925-932.
27. Demetri GD, von Mehren M, Blanke CD, et al. Efficacy and safety of imatinib mesylate in advanced gastrointestinal stromal tumors. N Engl J Med. 2002;347:472-480.
28. Antonescu CR, Besmer P, Guo T, et al. Acquired resistance to imatinib in gastrointestinal stromal tumor occurs through secondary gene mutation. Clin Cancer Res. 2005;11:4182-4190.
29. Bjornsti MA, Houghton PJ. The TOR pathway: a target for cancer therapy. Nat Rev Cancer. 2004;4:335-348.
30. Palacios R, Steinmetz M. IL-3-dependent mouse clones that express B-220 surface antigen, contain Ig genes in germ-line configuration, and generate B lymphocytes in vivo. Cell. 1985;41:727-734.
31. Feng SH, Tsai S, Rodriguez J, Lo SC. Mycoplasmal infections prevent apoptosis and induce malignant transformation of interleukin-3-dependent 32D hematopoietic cells. Mol Cell Biol. 1999;19:7995-8002.

32. Chambaud I, Wroblewski H, Blanchard A. Interactions between mycoplasma lipoproteins and the host immune system. Trends Microbiol. 1999;7: 493-499.
33. Chou TC, Talalay P. Quantitative analysis of dose-effect relationships: the combined effects of multiple drugs or enzyme inhibitors. Adv Enzyme Regul. 1984;22:27-55.
34. Mohi MG, Boulton C, Gu TL, et al. Combination of rapamycin and protein tyrosine kinase (PTK) inhibitors for the treatment of leukemias caused by oncogenic PTKs. Proc Natl Acad Sci U S A. 2004; 101:3130-3135.
35. Nakao M, Yokota S, Iwai T, et al. Internal tandem duplication of the flt3 gene found in acute myeloid leukemia. Leukemia. 1996;10:1911-1918.
36. Care RS, Valk PJ, Goodeve AC, et al. Incidence and prognosis of c-KIT and FLT3 mutations in core binding factor (CBF) acute myeloid leukaemias. Br J Haematol. 2003;121:775-777.
37. Martinez-Lorenzo MJ, Anel A, Monleon I, et al. Tyrosine phosphorylation of the p85 subunit of phosphatidylinositol 3-kinase correlates with high proliferation rates in sublines derived from the Jurkat leukemia. Int J Biochem Cell Biol. 2000;32: 435-445.
38. Chen X, Thakkar H, Tyan F, et al. Constitutively active Akt is an important regulator of TRAIL sensitivity in prostate cancer. Oncogene. 2001;20: 6073-6083.
39. Kandasamy K, Srivastava RK. Role of the phosphatidylinositol 3′-kinase/PTEN/Akt kinase pathway in tumor necrosis factor-related apoptosis-inducing ligand-induced apoptosis in non-small cell lung cancer cells. Cancer Res. 2002;62: 4929-4937.
40. Wang Q, Wang X, Hernandez A, Hellmich MR, Gatalica Z, Evers BM. Regulation of TRAIL expression by the phosphatidylinositol 3-kinase/Akt/GSK-3 pathway in human colon cancer cells. J Biol Chem. 2002;277:36602-36610.
41. Yuan XJ, Whang YE. PTEN sensitizes prostate cancer cells to death receptor-mediated and drug-induced apoptosis through a FADD-dependent pathway. Oncogene. 2002;21:319-327.
42. del Peso L, Gonzalez-Garcia M, Page C, Herrera R, Nunez G. Interleukin-3-induced phosphorylation of BAD through the protein kinase Akt. Science. 1997;278:687-689.
43. Blume-Jensen P, Janknecht R, Hunter T. The kit receptor promotes cell survival via activation of PI 3-kinase and subsequent Akt-mediated phosphorylation of Bad on Ser136. Curr Biol. 1998;8: 779-782.
44. Frost MJ, Ferrao PT, Hughes TP, Ashman LK. Juxtamembrane mutant V560GKit is more sensitive to imatinib (STI571) compared with wild-type c-kit whereas the kinase domain mutant D816VKit is resistant. Mol Cancer Ther. 2002;1: 1115-1124.
45. Beghini A, Bellini M, Magnani I, et al. STI 571 inhibition effect on KIT(Asn822Lys)-mediated signal transduction cascade. Exp Hematol. 2005;33: 682-688.
46. Mizuki M, Fenski R, Halfter H, et al. Flt3 mutations from patients with acute myeloid leukemia induce transformation of 32D cells mediated by the Ras and STAT5 pathways. Blood. 2000;96: 3907-3914.
47. Casteran N, De Sepulveda P, Beslu N, et al. Signal transduction by several KIT juxtamembrane domain mutations. Oncogene. 2003;22:4710-4722.
48. Ning ZQ, Li J, Arceci RJ. Signal transducer and activator of transcription 3 activation is required for Asp(816) mutant c-Kit-mediated cytokine-independent survival and proliferation in human leukemia cells. Blood. 2001;97:3559-3567.
49. O'Farrell AM, Ichihara M, Mui AL, Miyajima A. Signaling pathways activated in a unique mast cell line where interleukin-3 supports survival and stem cell factor is required for a proliferative response. Blood. 1996;87:3655-3668.
50. Jacobs-Helber SM, Penta K, Sun Z, Lawson A, Sawyer ST. Distinct signaling from stem cell factor and erythropoietin in HCD57 cells. J Biol Chem. 1997;272:6850-6853.
51. Growney JD, Clark JJ, Adelsperger J, et al. Activation mutations of human c-KIT resistant to imatinib mesylate are sensitive to the tyrosine kinase inhibitor PKC412. Blood. 2005;106:721-724.
52. Duensing A, Medeiros F, McConarty B, et al. Mechanisms of oncogenic KIT signal transduction in primary gastrointestinal stromal tumors (GISTs). Oncogene. 2004;23:3999-4006.
53. Bowman T, Garcia R, Turkson J, Jove R. STATs in oncogenesis. Oncogene. 2000;19:2474-2488.
54. de Groot RP, Raaijmakers JA, Lammers JW, Jove R, Koenderman L. STAT5 activation by BCR-Abl contributes to transformation of K562 leukemia cells. Blood. 1999;94:1108-1112.
55. Turkson J, Bowman T, Garcia R, Caldenhoven E, De Groot RP, Jove R. Stat3 activation by Src induces specific gene regulation and is required for cell transformation. Mol Cell Biol. 1998;18:2545-2552.
56. Salh B, Marotta A, Wagey R, Sayed M, Pelech S. Dysregulation of phosphatidylinositol 3-kinase and downstream effectors in human breast cancer. Int J Cancer. 2002;98:148-154.
57. Bagrintseva K, Geisenhof S, Kern R, et al. FLT3-ITD-TKD dual mutants associated with AML confer resistance to FLT3 PTK inhibitors and cytotoxic agents by overexpression of Bcl-x(L). Blood. 2005;105:3679-3685.
58. Paull TT, Rogakou EP, Yamazaki V, Kirchgessner CU, Gellert M, Bonner WM. A critical role for histone H2AX in recruitment of repair factors to nuclear foci after DNA damage. Curr Biol. 2000; 10:886-895.
59. Sarbassov DD, Guertin DA, Ali SM, Sabatini DM. Phosphorylation and regulation of Akt/PKB by the rictor-mTOR complex. Science. 2005;307:1098-1101.
60. Edinger AL, Linardic CM, Chiang GG, Thompson CB, Abraham RT. Differential effects of rapamycin on mammalian target of rapamycin signaling functions in mammalian cells. Cancer Res. 2003; 63:8451-8460.
61. Kindler T, Breitenbuecher F, Kasper S, et al. In BCR-ABL-positive cells, STAT-5 tyrosine-phosphorylation integrates signals induced by imatinib mesylate and Ara-C. Leukemia. 2003;17:999-1009.
62. Mol CD, Dougan DR, Schneider TR, et al. Structural basis for the autoinhibition and STI-571 inhibition of c-Kit tyrosine kinase. J Biol Chem. 2004; 279:31655-31663.
63. Ma Y, Cunningham ME, Wang X, Ghosh I, Regan L, Longley BJ. Inhibition of spontaneous receptor phosphorylation by residues in a putative alpha-helix in the KIT intracellular juxtamembrane region. J Biol Chem. 1999;274:13399-13402.
64. Tartaglia M, Niemeyer CM, Fragale A, et al. Somatic mutations in PTPN11 in juvenile myelomonocytic leukemia, myelodysplastic syndromes and acute myeloid leukemia. Nat Genet. 2003;34:148-150.
65. Kiyoi H, Ohno R, Ueda R, Saito H, Naoe T. Mechanism of constitutive activation of FLT3 with internal tandem duplication in the juxtamembrane domain. Oncogene. 2002;21:2555-2563.
66. Jin L, Asano H, Blau CA. Stimulating cell proliferation through the pharmacologic activation of c-kit. Blood. 1998;91:890-897.
67. Wandzioch E, Edling CE, Palmer RH, Carlsson L, Hallberg B. Activation of the MAP kinase pathway by c-Kit is PI-3 kinase dependent in hematopoietic progenitor/stem cell lines. Blood. 2004;104: 51-57.
68. Langford D, Hurford R, Hashimoto M, Digicaylioglu M, Masliah E. Signalling crosstalk in FGF2-mediated protection of endothelial cells from HIV-gp120. BMC Neurosci. 2005;6:8.